INTERNATIONAL JOURNAL FOR NUMERICAL AND ANALYTICAL METHODS IN GEOMECHANICS
Int. J. Numer. Anal. Meth. Geomech. 2006; **30**:577–597
Published online 8 December 2005 in Wiley InterScience (www.interscience.wiley.com). DOI: 10.1002/nag.491

Three-dimensional finite elements for the analysis of soil contamination using a multiple-porosity approach

Abbas El-Zein[*,†,¶], John P. Carter[‡,‖] and David W. Airey[§,**]

Centre for Geotechnical Research, University of Sydney, NSW 2006, Australia

SUMMARY

A three-dimensional finite-element model of contaminant migration in fissured clays or contaminated sand which includes multiple sources of non-equilibrium processes is proposed. The conceptual framework can accommodate a regular network of fissures in 1D, 2D or 3D and immobile solutions in the macro-pores of aggregated topsoils, as well as non-equilibrium sorption. A Galerkin weighted-residual statement for the three-dimensional form of the equations in the Laplace domain is formulated. Equations are discretized using linear and quadratic prism elements. The system of algebraic equations is solved in the Laplace domain and solution is inverted to the time domain numerically. The model is validated and its scope is illustrated through the analysis of three problems: a waste repository deeply buried in fissured clay, a storage tank leaking into sand and a sanitary landfill leaching into fissured clay over a sand aquifer. Copyright © 2005 John Wiley & Sons, Ltd.

KEY WORDS: advection–dispersion; finite element method; multiple-porosity; contaminant migration; Laplace transform

INTRODUCTION

The deterioration of the environmental indicators of many ecosystems has led, over the last two decades, to tighter environmental control and an increase in research into the fate of contaminants in soil, air and water. The ability of practitioners and regulators to predict the extent and rate of dispersion of pollution plumes can help them develop better pre-emptive or remedial strategies. For example, designers of landfills are often required by environmental authorities to demonstrate that groundwater concentrations of a set of pollutants will not

[*]Correspondence to: Abbas El-Zein, Department of Civil Engineering, Centre for Geotechnical Research, University of Sydney, NSW 2006, Australia.
[†]E-mail: aelzein@civil.usyd.edu.au
[‡]E-mail: J.Carter@civil.usyd.edu.au
[§]E-mail: D.Airey@civil.usyd.edu.au
[¶]Senior Lecturer.
[‖]Challis Professor.
[**]Associate Professor.

Contract/grant sponsor: Australian Research Council

Received 1 December 2004
Revised 1 September 2005
Accepted 1 October 2005

Copyright © 2005 John Wiley & Sons, Ltd.

exceed certain health standards for hundreds of years after closure [1, 2]. Given the long-term nature of such requirements, compliance can only be demonstrated through the use of state-of-the-art computer models, closely replicating fate processes.

Under the continuum conceptualization of soils, developed by Biot [3], mass-transfer equations of contamination are, at their simplest, a mathematical combination of the following processes: molecular diffusion, advection, sorption and biological or radioactive decay. Mass-conservation statements of these processes lead to a fairly standard form of the advection–dispersion equation. Biot's approach is based on average values of physical soil parameters at a macro-scale of a few centimetres. Therefore, it does not replicate heterogeneities at a smaller scale. For example, local variations in seepage velocities are accounted for by the inclusion of a coefficient of mechanical dispersion. In fissured soils, differential transport in the fissures and the intact soil matrix leads to a breakdown of the continuum assumption [4, 5]. In structured agricultural top-soils, both the large pores between aggregated soil lumps and the small pores of the soil play an important role in plume dispersion [6–8]. In the case of soils polluted by non-aqueous phase liquids, pollutants may linger in the soil's pores and act as additional sources injecting contaminants into the mobile solution travelling through the soil [9–11].

One approach to describing this problem consists of 'downscaling' the numerical model so as to represent structuring or fissuring as it is, within the continuum framework, with a spatially-varying porosity. The discrete-fracture method [12–14] follows this approach but requires a large amount of data and, sometimes, prohibitive computational resources. Another approach is to extend the continuum conceptualization into a bi-continuum one. In this approach, the fissures of damaged soils and the macro-pores of aggregated soils are included at every point of the model, in addition to the regular pores and the soil matrix. The method, known as dual-porosity, has been successfully applied to the modelling of groundwater flow (e.g. References [15, 16]) and mass transfer in soils (e.g. References [17, 18]).

A number of solutions of the three-dimensional advection–dispersion equation have been proposed [19–24]. However, only a handful of three-dimensional soil-contamination models, based on dual or multiple-porosity transport assumptions, are in the literature. Therrien and Sudicky [25] proposed a three-dimensional finite-element method (FEM) for fractured soils based on the discrete-fracture approach. Elzein and Booker [26] developed a boundary-element method (BEM) for multi-process non-equilibrium exchange, including immobile solutions in the pores acting as exchange sites with the mobile solution. Elzein [27] presented a boundary-element method for multiple-porosity transport, incorporating both fissured soils and immobile solutions in the fissures or the pores. Sudicky [28, 29] proposed a Laplace-transform finite element model for dual porosity media and presented results for problems in 1D and 2D. The model, however, did not incorporate non-equilibrium sorption. More generally, to the best of the authors' knowledge, no finite-element model of fissured soils using the multiple-porosity concept in 3D can be found in the literature.

This paper proposes a three-dimensional Galerkin finite-element method in the Laplace domain based on a multiple-porosity conceptualization of the soils developed earlier by the authors [30–32]. The novelty of the proposed formulation lies in its ability to model concurrently, multiple sources of non-equilibrium processes and transport through fissures. Although the Laplace transform limits the method to problems in which groundwater flow is steady-state, it removes the need for time stepping and increases the Peclet-number limit of problems at which numerical dispersion becomes important [33]. In addition, the proposed

Copyright © 2005 John Wiley & Sons, Ltd.

method can solve a wide range of contamination problems in 3D space, including intact soils, soils with regular fissure networks, soils with multiple sources of non-equilibrium sorption and soils with immobile solutions in the pores.

MULTIPLE-POROSITY MASS TRANSFER

The conceptual model presented here focuses on mass transfer. Fluid flow is assumed to be steady-state but will not be explicitly presented. Three compartments for dissolved contaminants are included in the conceptual model (POROS) [30]: a primary compartment for advection–dispersion transport with non-equilibrium sorption, a secondary compartment with diffusion and linear sorption in rectangular or spherical soil blocks, and a tertiary compartment of immobile solutions (see Figure 1). The secondary compartment can represent the intact soil matrix in a fissured soil or aggregated soil in structured media. Exchange between the secondary compartment, on the one hand, and the primary and tertiary compartments, on the other hand, follows a linear hereditary process. Exchange between the primary and tertiary compartments is represented by a first-order, rate-limited equation. The conceptual model can therefore be adapted to represent three general types of contaminant migration problems: (a) fissured or structured soils, (b) non-equilibrium sorption, (c) immobile solutions in dead-end pores. The model can also represent the conventional problem of contaminants

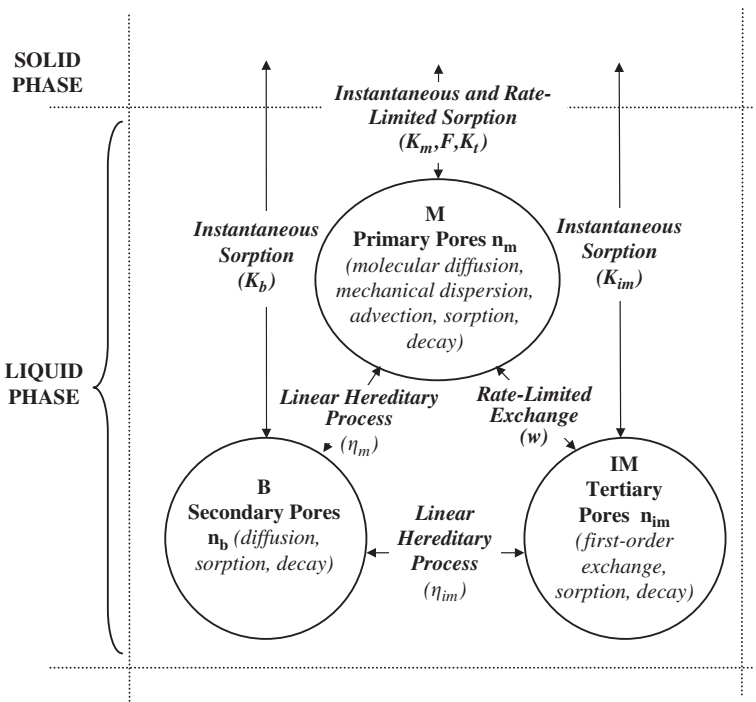

Figure 1. Multiple-porosity conceptual framework.

Copyright © 2005 John Wiley & Sons, Ltd.

travelling through intact soils with instantaneous sorption. A mass conservation statement can be written for each of the three primary, secondary and tertiary compartments

$$\nabla[\mathbf{v}_a c_\mathrm{m} - \nabla(\mathbf{D}_a c_\mathrm{m})] + n_\mathrm{m} R^i_\mathrm{m} \frac{\partial c_\mathrm{m}}{\partial t} + \phi_\mathrm{m} \frac{\partial q^\mathrm{ne}_\mathrm{m}}{\partial t} + n_\mathrm{m} \lambda_\mathrm{m} c_\mathrm{m} + w(c_\mathrm{m} - c_\mathrm{im}) + f^\mathrm{b}_\mathrm{m} = 0 \tag{1}$$

$$n_\mathrm{b} R^i_\mathrm{b} \frac{\partial c_\mathrm{b}}{\partial t} - D_\mathrm{b} \nabla^2 c_\mathrm{b} + n_\mathrm{b} \lambda_\mathrm{b} c_\mathrm{b} + f^\mathrm{m}_\mathrm{b} + f^\mathrm{im}_\mathrm{b} = 0 \tag{2}$$

$$n_\mathrm{im} R^i_\mathrm{im} \frac{\partial c_\mathrm{im}}{\partial t} + n_\mathrm{im} \lambda_\mathrm{im} c_\mathrm{im} + f^\mathrm{b}_\mathrm{im} - w(c_\mathrm{m} - c_\mathrm{im}) = 0 \tag{3}$$

where t is time; x_j[L] ($j = 1, 3$) is a co-ordinate system; subscripts m, b and im refer to primary (mobile solution), secondary (soil-matrix blocks) and tertiary (immobile solutions) compartments, respectively; $c_\mathrm{m}(t, x_j), c_\mathrm{b}(t, x_j)$ and $c_\mathrm{im}(t, x_j)$ [M L^{-3}] are the contaminant concentrations; $\mathbf{v}_a$ [L T^{-1}] is the vector (v_{a1}, v_{a2}, v_{a3}) of Darcy velocity in the primary compartment resulting from the three components V_1, V_2 and V_3 [L T^{-1}] of seepage velocity in the three directions; $\mathbf{D}_a$ [L^2 T^{-1}] is the 'effective' tensor of hydrodynamic dispersion in the primary compartment, D_{a1}, D_{a2} and D_{a3} are its diagonal components, and $D_{a12}, = D_{a21}, D_{a13} = D_{a31}$, and $D_{a23} = D_{a32}$, its non-diagonal components; D_b [L^2 T^{-1}] is the coefficient of molecular diffusion in the secondary compartment; n is the soil porosity of the primary and tertiary compartments; n_sb is the porosity of the secondary compartment; $S_\mathrm{m}, S_\mathrm{b}$ and S_im are the degrees of saturation of the primary, secondary and tertiary compartments, respectively; $n_\mathrm{m} = S_\mathrm{m} n$, $n_\mathrm{im} = S_\mathrm{im} n$ are the effective porosities of the primary and tertiary compartments; $n_\mathrm{b} = S_\mathrm{b} n_\mathrm{sb}$ is the effective porosity of the secondary compartment; $\lambda_\mathrm{m}, \lambda_\mathrm{b}$ and λ_im [T^{-1}] are decay coefficients; $q^\mathrm{ne}_\mathrm{m}(t, x_j)$ is the concentration of contaminant sorbed under non-equilibrium conditions, expressed in units of [M M^{-1}] if the primary compartment is made of intact soil and units of [M L^{-2}] if it represents fissures and sorption is occuring against the fissure walls; ϕ_m is the soil dry density [M L^{-3}] if the primary compartment is made of intact soil, and the surface area per unit volume [L^{-1}] if it refers to fissures; $R^i_\mathrm{m}, R^i_\mathrm{b}$ and R^i_im are the instantaneous linear sorption retardation factors, w [T^{-1}] is the first-order mass transfer coefficient between the primary and tertiary compartments, $f^\mathrm{b}_\mathrm{m} = -f^\mathrm{m}_\mathrm{b}$ [M L^{-3} T^{-1}] is the rate of exchange between the primary and secondary compartments, and $f^\mathrm{b}_\mathrm{im} = -f^\mathrm{im}_\mathrm{b}$ [M L^{-3} T^{-1}] is the rate of exchange between the tertiary and secondary compartments.

An additional equation for non-equilibrium sorption in the primary compartment can be written as follows:

$$\frac{\partial q^\mathrm{ne}_\mathrm{m}}{\partial t} = k_t\{(1 - F) q^\mathrm{e}_\mathrm{m} - q^\mathrm{ne}_\mathrm{m}\} - \lambda_\mathrm{s} q^\mathrm{ne}_\mathrm{m} \tag{4}$$

where $q^\mathrm{e}_\mathrm{m}(x_j)$ [M M^{-1}] is the concentration of sorbed contaminant at equilibrium, k_t [T^{-1}] is the first-order sorption rate constant in the primary compartment, F is the proportion of instantaneous sorption in the primary compartment, λ_s is the decay coefficient for the sorbed phase.

The instantaneous retardation factors can be expressed in terms of the total retardation factors $R_\mathrm{m}, R_\mathrm{b}$ and R_im as follows: $R^i_\mathrm{m} = 1 + F(R_\mathrm{m} - 1), R^i_\mathrm{b} = R_\mathrm{b}$ and $R^i_\mathrm{im} = R_\mathrm{im}$.

Exchange between the secondary compartment, on the one hand, and the primary and tertiary compartments on the other hand, are governed by a linear hereditary process, according

Copyright © 2005 John Wiley & Sons, Ltd.

to the following equations:

$$f_{\mathrm{m}}^{\mathrm{b}} = c_{\mathrm{m0}}\eta_{\mathrm{m}}(t) + \int_0^t \eta_{\mathrm{m}}(t-\tau)\frac{\partial c_{\mathrm{m}}(\tau)}{\partial \tau}\,\mathrm{d}\tau \tag{5}$$

$$f_{\mathrm{im}}^{\mathrm{b}} = c_{\mathrm{im0}}\eta_{\mathrm{im}}(t) + \int_0^t \eta_{\mathrm{im}}(t-\tau)\frac{\partial c_{\mathrm{im}}(\tau)}{\partial \tau}\,\mathrm{d}\tau \tag{6}$$

where η_{m} and η_{im} are exchange parameters which can be derived analytically under certain simplifying assumptions; c_{m0} and c_{im0} are respective values of c_{m} and c_{im} at time $t = 0$.

A general form of a set of boundary conditions for Equation (1) is given by

$$\alpha c_{\mathrm{m}} + \beta f_{\mathrm{mn}} = \varphi \tag{7}$$

where f_{mn} is the flux of contaminant normal to the boundary in the primary compartment and α, β and φ are given coefficients.

Application of the Laplace-transform

$$\bar{g}(s) = \int_0^\infty \mathrm{e}^{-st} g(t)\,\mathrm{d}t \tag{8}$$

to Equations (1)–(4), where s is the Laplace parameter, removes the time derivatives from the governing equations. These equations can then be manipulated to derive a boundary-value differential equation for the Laplace transform of contaminant concentration in the primary compartment, $\bar{c}_{\mathrm{m}}$. Combining the Laplace transforms of Equations (1)–(7), the following formulation is obtained:

$$\nabla(\mathbf{D}_a \nabla \bar{c}_{\mathrm{m}}) - \mathbf{v}_a \nabla \bar{c}_{\mathrm{m}} = \bar{\Phi}_{\mathrm{m}} \bar{c}_{\mathrm{m}} - \bar{\Phi}_{\mathrm{m0}} c_{\mathrm{m0}} \tag{9}$$

$$\bar{c}_{\mathrm{im}} = \bar{A}_{\mathrm{im}} \bar{c}_{\mathrm{m}} + \bar{B}_{\mathrm{im}} c_{\mathrm{m0}} \tag{10}$$

$$\bar{q}_{\mathrm{m}}^{\mathrm{ne}} = \bar{A}_{\mathrm{ne}} \bar{c}_{\mathrm{m}} \tag{11}$$

$$\bar{q}_{\mathrm{m}}^{\mathrm{e}} = n_{\mathrm{m}}(R_{\mathrm{m}} - 1)\bar{c}_{\mathrm{m}} \tag{12}$$

$$\bar{q}_{\mathrm{im}}^{\mathrm{e}} = n_{\mathrm{im}}(R_{\mathrm{im}} - 1)\bar{c}_{\mathrm{im}} \tag{13}$$

$$\alpha \bar{c}_{\mathrm{m}} + \beta \bar{f}_{\mathrm{mn}} = \frac{\varphi}{s} \tag{14}$$

where

$$\bar{\Phi}_{\mathrm{m}} = (n_{\mathrm{m}} \bar{r}_{\mathrm{m}} + \bar{A}_{\mathrm{ne}})s + w(1 - \bar{A}_{\mathrm{im}}) + n_{\mathrm{m}}\lambda_{\mathrm{m}} + \bar{\eta}_{\mathrm{m}}\lambda_{\mathrm{b}} \tag{15}$$

$$\bar{\Phi}_{\mathrm{m0}} = n_{\mathrm{m}} \bar{r}_{\mathrm{m}} + w\bar{B}_{\mathrm{im}} \tag{16}$$

$$\bar{A}_{\mathrm{im}} = \frac{w}{n_{\mathrm{im}} \bar{r}_{\mathrm{im}} s + w + n_{\mathrm{im}}\lambda_{\mathrm{im}} + \lambda_{\mathrm{b}}\bar{\eta}_{\mathrm{im}}} \tag{17}$$

Copyright © 2005 John Wiley & Sons, Ltd.

$$\bar{B}_{\mathrm{im}} = \frac{n_{\mathrm{im}}\bar{r}_{\mathrm{im}}}{w}\bar{A}_{\mathrm{im}} \tag{18}$$

$$\bar{A}_{\mathrm{ne}} = \frac{n_{\mathrm{m}}k_t(1-F)(R_{\mathrm{m}}-1)}{s+k_t} \tag{19}$$

$$\bar{r}_{\mathrm{m}} = R^i_{\mathrm{m}} + \frac{\bar{\eta}_{\mathrm{m}}}{n_{\mathrm{m}}} \tag{20}$$

$$\bar{r}_{\mathrm{im}} = R^i_{\mathrm{im}} + \frac{\bar{\eta}_{\mathrm{im}}}{n_{\mathrm{im}}} \tag{21}$$

where $q^{\mathrm{e}}_{\mathrm{im}}(x_j)$ is the concentration of sorbed contaminant at equilibrium in the tertiary compartment.

To model fissured media using the above formulation, the soil is assumed to be made of $n_{\mathrm{f}}(=1,2 \text{ or } 3)$ orthogonal fissure planes in between rectangular soil-matrix blocks of dimensions H_1, H_2 and H_3 in the three directions, respectively. The widths of the fissure openings are h_1, h_2 and h_3 in the three directions. If the fissures are identified with the primary compartments, and the intact soil blocks with the secondary compartments, analytical expressions of $\bar{\eta}_{\mathrm{m}}$ and $\bar{\eta}_{\mathrm{im}}$ can be derived by using the Boltzmann superposition principle and continuity conditions at the interface between a fissure plane and the adjacent soil-matrix blocks [33, 34]. These expressions are given in Appendix A. Structured soils can also be modelled, if the secondary and primary compartments are made to represent, respectively, a set of spherical lenses of radius r_0 and the macro-pores between them. Exchange parameters $\bar{\eta}_{\mathrm{m}}$ and $\bar{\eta}_{\mathrm{im}}$ for this case are also given in Appendix A [35].

Table I shows the types of problems that can be solved with the above formulation, including definitions of compartments and key parameters. Next, a three-dimensional finite-element solution of Equations (9)–(14) is presented.

GALERKIN WEIGHTED-RESIDUAL STATEMENT

A Galerkin weighted-residual statement of Equation (9) can be written as follows:

$$\int_{\Omega} N_i(x_j)\{\nabla(D_a\nabla\bar{c}_{\mathrm{m}}) - v_a\nabla\bar{c}_{\mathrm{m}} - \bar{\Phi}_{\mathrm{m}}\bar{c}_{\mathrm{m}}\}\,\mathrm{d}\Omega = 0 \tag{22}$$

where Ω is the domain of the problem and $N_i(x_j)$ are the interpolation functions of the elements, used as weighting functions in the residual statement. Initial concentration of contaminants is assumed to be identically zero in Equation (22) for the sake of simplicity. However, non-zero initial concentrations can be easily incorporated. Dispersion coefficients are taken to be uniform over each element, although they can vary from one element to the next. Integrating by parts and discretizing Equation (22), we can write

$$\sum_{e=1}^{E}\left\langle \int_{\Omega_e} ([B_e]^{\mathrm{T}}[D_e][B_e] - [B_e]^{\mathrm{T}}[V_e][N_e] + \bar{\Phi}_{\mathrm{m}}\{N_e\}\{N_e\}^{\mathrm{T}})\{\bar{c}_{\mathrm{me}}\}\,\mathrm{d}\Omega_e \right\rangle$$
$$+ \sum_{e=1}^{E}\left\langle \int_{\Omega_e} (\{N_e\}^{\mathrm{T}}\{\bar{Q}_e\})\,\mathrm{d}\Omega_e \right\rangle = 0 \tag{23}$$

Copyright © 2005 John Wiley & Sons, Ltd.

Copyright © 2005 John Wiley & Sons, Ltd.

Table I. Problem types and compartments definitions (adapted from earlier table by the authors [30]).

Problem type		Problem description	Primary compartment	Secondary compartment	Tertiary compartment	Key parameters
Type I: intact soils	A	With linear sorption	Pores of intact soil	NON-EXISTENT	NON-EXISTENT	$h_1 = h_2 = h_3 = 0$ $F = 1$ $n_{im} = 0$ $r_0 = 0$
Type II: intact soils with non-equilibrium	B	With non-equilibrium sorption	Pores of intact soil	NON-EXISTENT	NON-EXISTENT	$h_1 = h_2 = h_3 = 0$ $F < 1$ $n_{im} = 0$ $r_0 = 0$
	C	With multiple non-equilibrium processes	Pores of intact soil	NON-EXISTENT	Immobile solutions in pores of intact soil	$h_1 = h_2 = h_3 = 0$ $F < 1$ $n_{im} > 0$ $r_0 = 0$
Type III: fissured soils	E	Fissure network	Fissures	Soil-matrix blocks with diffusion and linear sorption	NON-EXISTENT	$h_1, h_2, h_3 > 0$ $F = 1$ $n_{im} = 0$ $r_0 = 0$
	F	Fissure network	Fissures	NON-EXISTENT	Soil-matrix pores	$h_1 = h_2 = h_3 = 0$ $F = 1$ $n_{im} > 0$ $r_0 = 0$
	G	Fissure network with multiple non-equilibrium processes	Fissures	Soil-matrix blocks with diffusion and linear sorption	Immobile solutions in fractures	$h_1, h_2, h_3 > 0$ $F < 1$ $n_{im} > 0$ $r_0 = 0$
Type IV: structured soils	H	Structured soil	Macro-pores	Soil-matrix spherical pores	NON-EXISTENT	$h_1 = h_2 = h_3 = 0$ $F = 1$ $n_{im} = 0$ $r_0 > 0$
	I	Structured soil	Macro-pores	NON-EXISTENT	Soil-matrix	$h_1 = h_2 = h_3 = 0$ $F = 1$ $n_{im} > 0$ $r_0 = 0$
	J	Structured soil with multiple non-equilibrium processes	Macro-pores	Soil-matrix spherical pores	Immobile solutions in macro-pores	$h_1 = h_2 = h_3 = 0$ $F < 1$ $n_{im} > 0$ $r_0 > 0$

where subscript e refers to the eth element, E is the total number of elements, n_e is the number of nodes in element e, Ω_e is the volume of element e

$$\{N_e\} = \begin{Bmatrix} N_1 \\ N_2 \\ \vdots \\ N_{n-1} \\ N_n \end{Bmatrix} \quad (n_e \times 1) \tag{24}$$

$$[B_e] = \begin{bmatrix} \left\{\dfrac{\partial\{N_e\}}{\partial x_1}\right\}^{\mathrm{T}} \\ \left\{\dfrac{\partial\{N_e\}}{\partial x_2}\right\}^{\mathrm{T}} \\ \left\{\dfrac{\partial\{N_e\}}{\partial x_3}\right\}^{\mathrm{T}} \end{bmatrix} \quad (3 \times n_e) \tag{25}$$

$$[N_e] = \begin{bmatrix} \{N_e\}^{\mathrm{T}} \\ \{N_e\}^{\mathrm{T}} \\ \{N_e\}^{\mathrm{T}} \end{bmatrix} \quad (3 \times n_e) \tag{26}$$

$$[D_e] = \begin{bmatrix} D_{a1} & D_{a12} & D_{a13} \\ D_{a21} & D_{a2} & D_{a23} \\ D_{a31} & D_{a32} & D_{a3} \end{bmatrix} \quad (3 \times 3) \tag{27}$$

$$[V_e] = \begin{bmatrix} v_{a1} & 0 & 0 \\ 0 & v_{a2} & 0 \\ 0 & 0 & v_{a3} \end{bmatrix} \quad (3 \times 3) \tag{28}$$

$\{\bar{c}_{\mathrm{me}}\}$ is the vector of Laplace-transformed nodal concentrations for element e and $\{\bar{Q}_e\}$ is a nodal vector of contaminant sources in the Laplace domain.

Two types of three-dimensional elements have been implemented: eight-noded (P8) and twenty-noded (P20) prisms [36]. The shape functions of both elements are linear. The interpolation functions of P8 are linear while those of P20 are parabolic. Enforcing boundary conditions, introducing a global vector of nodal concentrations $\{\bar{c}_{\mathrm{mg}}\}$ and re-arranging Equation (23), a linear algebraic system of equations of the following form is obtained:

$$([\bar{M}_0] + [\bar{M}_1])\{\bar{c}_{\mathrm{mg}}\} = \{\bar{r}\} \tag{29}$$

where $[\bar{M}_1]$, but not $[\bar{M}_0]$, is a function of $\bar{\Phi}_{\mathrm{m}}$. The system of Equations (29) is solved and the solution is inverted into the time domain numerically [37]. Matrix $[\bar{M}_0]$ needs to be evaluated

Copyright © 2005 John Wiley & Sons, Ltd.

only once, while $[\bar{M}_1]$ is re-assembled for each new value of the Laplace parameter because $\bar{\Phi}_m$ is a function of the Laplace parameter s. The algorithm is implemented in a FORTRAN computer program, CONFEM-3D, on a Pentium IV computer.

RESULTS

Validation

A number of problems, for which independent analytical or numerical solutions can be found, have been analysed using the proposed method. A wide variety of such 1D and 2D problems, which can also be modelled in 3D space, is available in the literature. For strictly three-dimensional problems, a boundary-element program, CONTAN, is used to validate the proposed method [26]. Excellent agreement with finite-element predictions is obtained. Three problems are now used to illustrate the validity of the method and its scope. The data for the three problems are given in Table II. Note that contaminants have been assumed to be non-decaying.

Table II. Data for three soil contamination problems.

		Problem 1 (waste repository deeply buried in soil)	Problem 2 (underground storage tank with multiple non-equilibrium processes)		Problem 3 (leaching from a sanitary landfill)
Parameters	Units	Fissured clay	Problem 2a: intact sand	Problem 2b: structured sand	Fissured clay over sand aquifer
H_1, H_2, H_3	m	0.1, 0.1, 0.1	NA	NA	0.1, 0.1, 0.1
h_1, h_2, h_3	m	0.001, 0.001, 0.001	NA	NA	0.001, 0.001, 0.001
R_0	m	NA	NA	0.02	NA
D_{a1}	$m^2\ s^{-1}$	1.902×10^{-10}	1.620×10^{-5}	1.620×10^{-5}	9.513×10^{-11}
D_{a2}	$m^2\ s^{-1}$	9.513×10^{-11}	3.240×10^{-6}	3.240×10^{-6}	4.755×10^{-10}
D_{a3}	$m^2\ s^{-1}$	9.513×10^{-11}	3.240×10^{-6}	3.240×10^{-6}	9.513×10^{-11}
v_{a1}	$m\ s^{-1}$	9.513×10^{-11}	3.240×10^{-6}	3.240×10^{-6}	0
v_{a2}	$m\ s^{-1}$	0	0	0	-9.513×10^{-11}
v_{a3}	$m\ s^{-1}$	0	0	0	0
n_m	ND	0.03	0.28	0.28	0.03
n_{im}	ND	0	0.07	0.07	0
R_m	ND	1	7.07	7.07	1
R_{im}	ND	1	25.29	25.29	1
w	s^{-1}	NA	5.787×10^{-8}	5.787×10^{-8}	NA
k_t	s^{-1}	NA	5.787×10^{-8}	5.787×10^{-8}	NA
F	ND	1	0.7	0.7	1
n_b	ND	0.4	NA	0.35	0.4
D_b	$m^2\ s^{-1}$	3.171×10^{-12}	NA	3.240×10^{-6}	3.171×10^{-10}
R_b	ND	1	NA	5.86	1
$\lambda_m, \lambda_b, \lambda_{im}, \lambda_s$	s^{-1}	0	0	0	0

NA: Not Applicable; ND: Dimensionless.

Copyright © 2005 John Wiley & Sons, Ltd.

Problem 1: deeply-buried waste repository in fissured clay

A cubic waste repository of dimensions $L_{x1} = L_{x2} = L_{x3} = 1$ m is leaking into the surrounding fissured clay (Figure 2(a)). The fissure network is three-dimensional, with fracture openings of 1 mm in between soil-matrix blocks that are 10 cm in size in all three directions. The concentration of pollutant in the repository is assumed to be constant at 1000 mg/l. Groundwater flows in the x_1 direction. A convergence analysis has been conducted and results have been compared to converged boundary-element predictions. The densest finite-element mesh used in the simulation is shown in Figure 2(b). Both P8 and P20 polynomial elements have been tested. Figure 3 shows the concentration profile in the x_1 direction. Very good agreement between the two methods is clearly obtained. Results from an equivalent two-dimensional boundary element analysis are shown, in which the dimension of the repository in the x_3

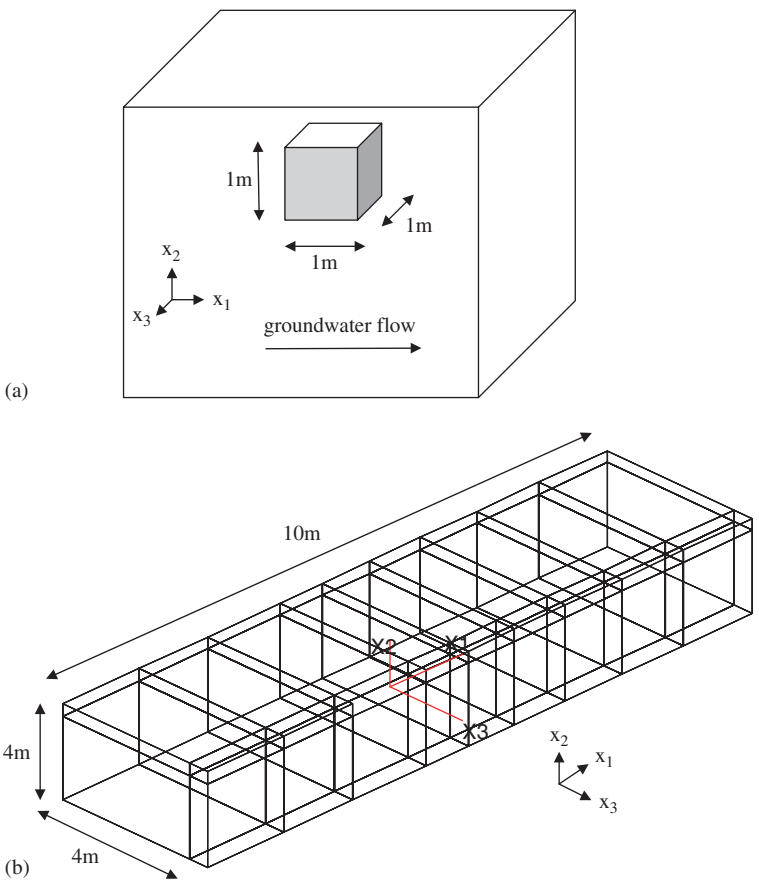

Figure 2. Problem 1: cubic waste repository in an infinite soil (figures not to scale): (a) perspective view; and (b) finite-element mesh, 35 elements (symmetries with respect to x_1–x_2 and x_1–x_3 planes have been used; the origin of the axes is at the centre of the repository; adjacent elements in the x_1 direction are graded at a ratio of $n = 1.1$; 6 rows of elements are used in the positive x_1 direction which coincides with groundwater flow and 2 rows of elements are used in the negative x_1 direction).

Copyright © 2005 John Wiley & Sons, Ltd.

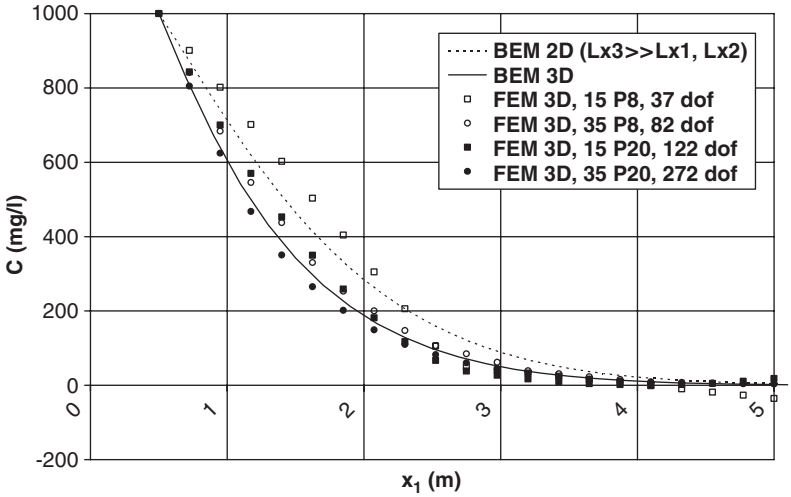

Figure 3. Problem 1: contamination profile after 100 years along the x_1-axis ($x_2 = x_3 = 0$) in the direction of groundwater flow, starting from the edge of the repository at $x_1 = 0.5$ m (dof: degrees of freedom).

direction is much greater than that of x_1 and x_2. Comparing curves from both sets of analyses, it is clear that, as expected, the two-dimensional analysis yields conservative results. However, the difference between two-dimensional and three-dimensional predictions can reach 30% at some points of the profile.

Problem 2: storage tank in a sandy soil with multiple non-equilibrium processes

An underground storage tank is leaking into the surrounding sand (Figure 4). The concentration of contaminant in the tank is assumed to be constant at C_0. The contaminant undergoes both instantaneous (70%) and time-dependent (30%) sorption. In addition, 20% of the soil's pores contain immobile solutions. Two versions of the problem are analysed. In the first case (problem 2a), the medium is a porous sand. In the second case (problem 2b), the sand is structured.

The purpose of the analysis of problem 2a is to study the effect of the orientation of the storage tank on the speed of contamination. Hence two designs are compared. In the first design ($D1$), the dimensions of the tank are $8 \times 2 \times 2\,\mathrm{m}^3$, while in the second design ($D2$), the tank is rotated around the x_2 axis by 90° and the dimensions become $2 \times 2 \times 8\,\mathrm{m}^3$. The direction of groundwater flow is in the x_1 co-ordinate direction in both cases.

A preliminary convergence analysis is carried out to validate predictions and determine the required degree of refinement of the mesh. Finite-element results are compared to three-dimensional boundary-element predictions. Results are shown in Figures 5(a) and (b). The finite-element mesh used in the final analyses is shown in Figure 5(c).

To highlight the effects of sorption and non-equilibrium processes, three additional analyses have been performed by modifying the data for problem 2a in the following way: (a) no sorption ($R_\mathrm{m} = R_\mathrm{im} = 1$), (b) pores contain mobile solution only ($n_\mathrm{im} = 0$), (c) all sorption is instantaneous ($F = 1$). Results are shown in Figure 6(a). As expected, the assumption of

Copyright © 2005 John Wiley & Sons, Ltd.

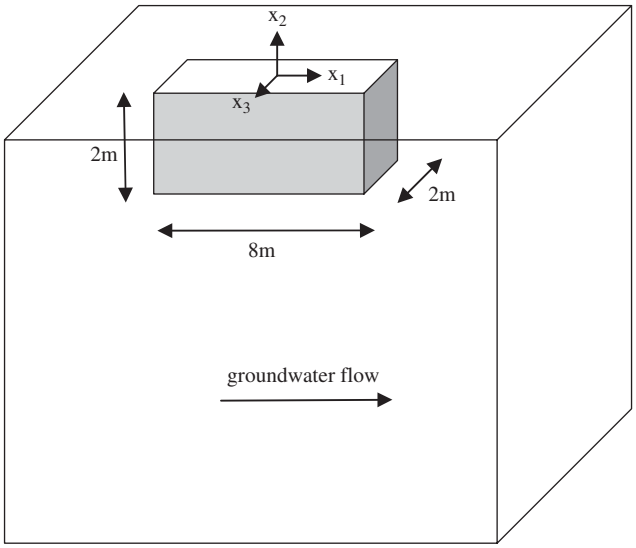

Figure 4. Problem 2: storage tank in a sandy soil (figures not to scale; centre of axes is at the centre of the top face of the tank).

instantaneous sorption yields slower transport compared to time-dependent sorption, the importance of which clearly increases with groundwater velocity. The existence of immobile solutions that act as storage sites for contaminants, leads to smaller concentrations in the mobile solution of the soil.

Figures 6(b) and (c) show the effects of the orientation of the storage tank on pollution profiles. Clearly, for the same time station, contamination reaches further in the case of $D1$ than $D2$, in both the x_1 and x_2 directions. Setting the largest side of the storage tank at a right angle to the direction of the groundwater flow might therefore reduce contamination downstream. In the case of $D2$, a two-dimensional analysis is likely to yield accurate results because the dimension of the tank along the x_3-axis is larger than its dimensions in the x_1 and x_2 directions. However, in the case of $D1$, a three-dimensional analysis is clearly necessary.

Next, results for problem 2b are shown. This case illustrates the capability of the new formulation in analysing a three-compartment problem, with transport in macro-pores, non-equilibrium sorption, exchange with immobile solutions in the macro-pores, as well as exchange with spherical macro-particles. The purpose of the analysis is to study the effect of changing the rate of exchange, D_b, between the macro-pore solution and the spherical aggregates. Figures 7(a) and (b) show contaminant profiles along the x_1 and x_2 direction, respectively. Exchange between the macro-pore solution and the aggregates reduces the contaminant concentration in the former and retards transport. As D_b decreases, the exchange process becomes so slow that exchange no longer occurs in practice and further reductions in D_b no longer have an effect on the results. As D_b increases, a point is reached where exchange is practically instantaneous and further increases in D_b makes no difference to concentration profiles, as the full storage capacity of the aggregates is reached. Hence, an 'active' interval of D_b values between 10^{-8} and 10^{-12} $m^2\,s^{-1}$ can be discerned in Figures 7 and 8. Clearly, the 'active' interval will depend on the particular time at which the solution is sought and the radius R_0 of the aggregates.

Copyright © 2005 John Wiley & Sons, Ltd.

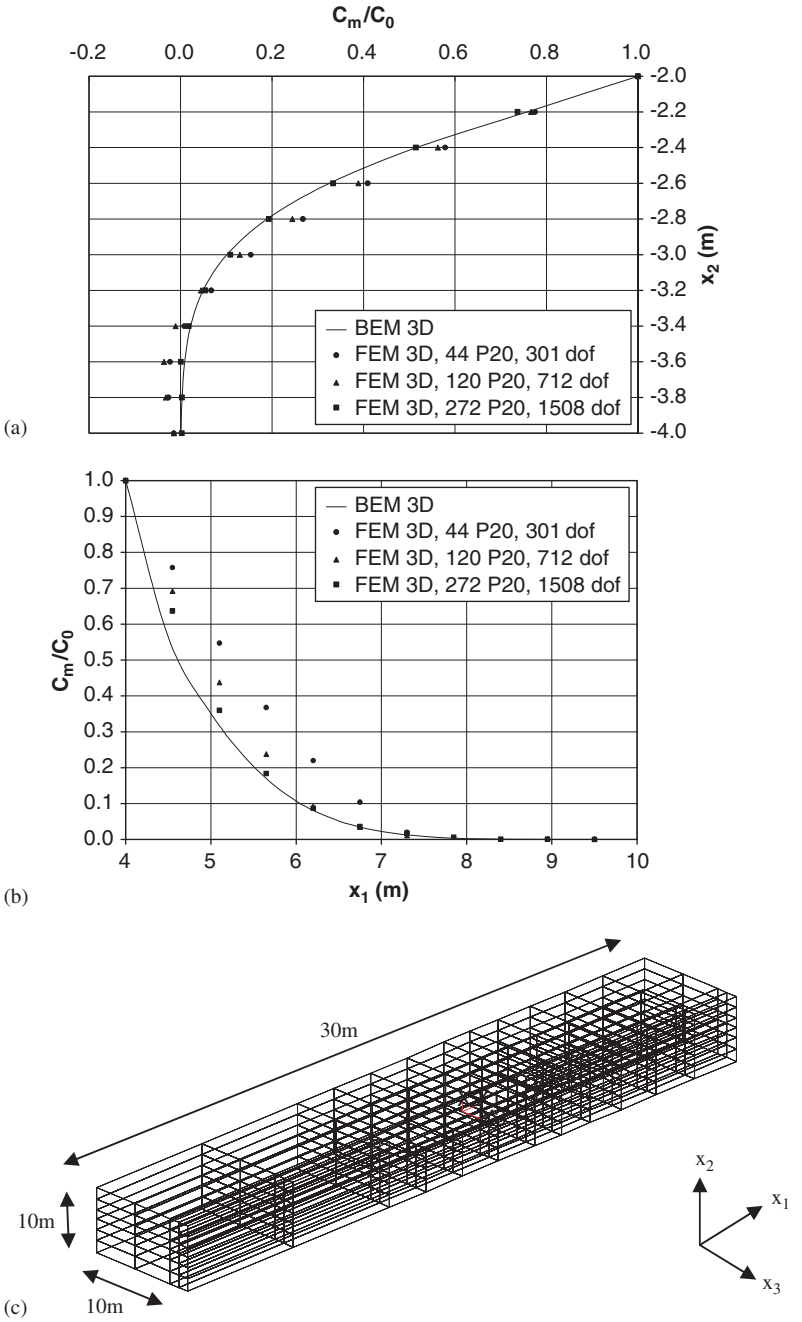

Figure 5. Problem 2a: convergence of the finite-element method (all profiles are at $t = 1$ day): (a) vertical concentration profile at $x_1 = x_2 = 0$; (b) horizontal concentration profile at $x_2 = -2$ m, $x_3 = 0$; and (c) finite-element mesh used in the final analyses (symmetry with respect to the x_1–x_2 plane has been used; 272 P20 elements, 1508 degrees of freedom; grading factor of 1.1 away from the storage tank in all three directions).

Copyright © 2005 John Wiley & Sons, Ltd.

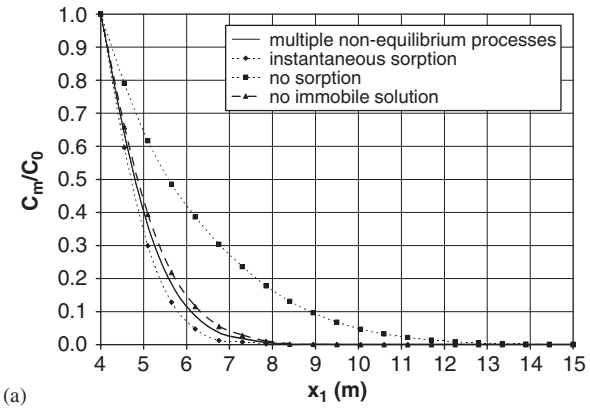

(a)

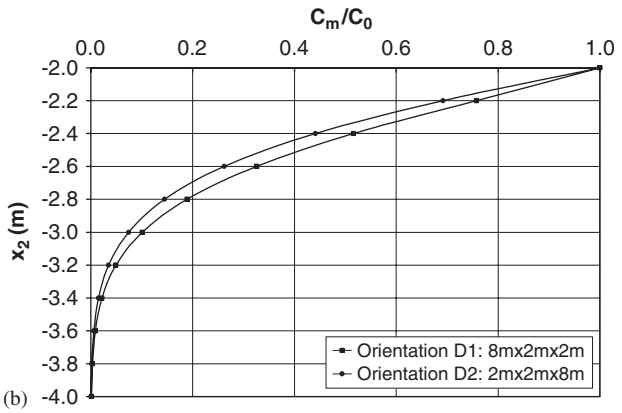

(b)

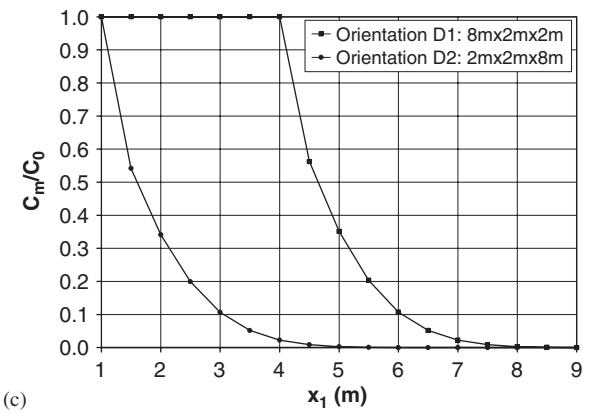

(c)

Figure 6. Problem 2a: effects of non-equilibrium processes and orientation of tank on concentration profiles after 1 day: (a) effects of sorption and non-equilibrium processes on horizontal profiles at $x_2 = -2$ m, $x_3 = 0$; (b) effect of orientation of tank on vertical profile at $x_1 = x_2 = 0$; and (c) effect of orientation of tank on horizontal profile at $x_2 = -2$ m, $x_3 = 0$.

Copyright © 2005 John Wiley & Sons, Ltd.

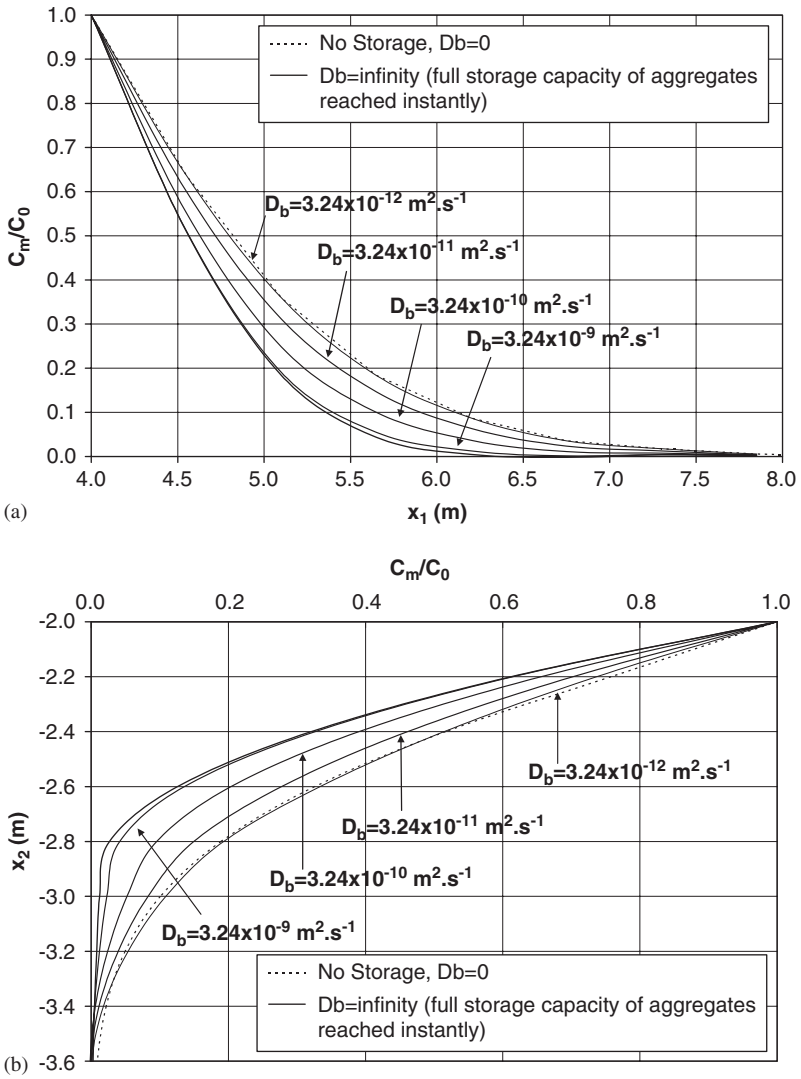

Figure 7. Problem 2b, effects of rate of diffusion into macro-particles, D_b on concentration profiles: (a) C_m/C_0 versus x_1, at $x_2 = -2$ m, $x_3 = 0$, $t = 1$ day; and (b) C_m/C_0 versus x_2, at $x_1 = x_3 = 0$, $t = 1$ day.

Problem 3: landfill leachate in a fissured clay

A sanitary landfill, 4 m deep, has been built over fissured clay (see Figure 8). The clay overlies a sandy aquifer, 12 m below the ground surface. The finite-element method is especially suitable for the solution of this problem because of its high surface area to volume ratio which reduces the effectiveness of the boundary-element method. For the purpose of the analysis, groundwater speed in the aquifer is assumed to be high and concentrations of pollutant at the interface

Copyright © 2005 John Wiley & Sons, Ltd.

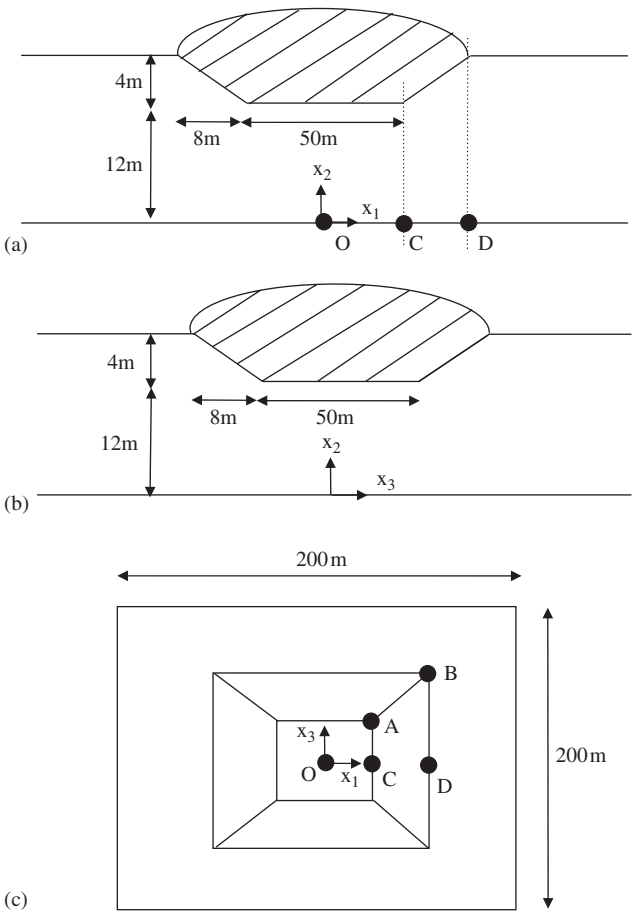

Figure 8. Problem 3: landfill leachate (figures not to scale): (a) cross-sectional view x_1–x_2; (b) cross-sectional view x_2–x_3; and (c) top view x_1–x_3.

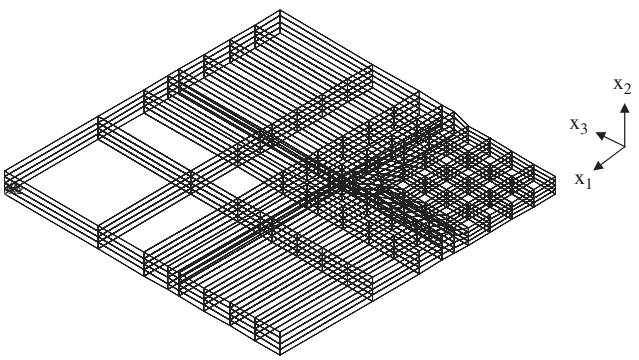

Figure 9. Problem 3: finite-element mesh (symmetries with respect to x_1–x_2 and x_2–x_3 planes have been used; 288 P20 elements, 1273 degrees of freedom; grading factor of 2 away from the landfill in the x_1 and x_3 directions; figure not to scale).

Copyright © 2005 John Wiley & Sons, Ltd.

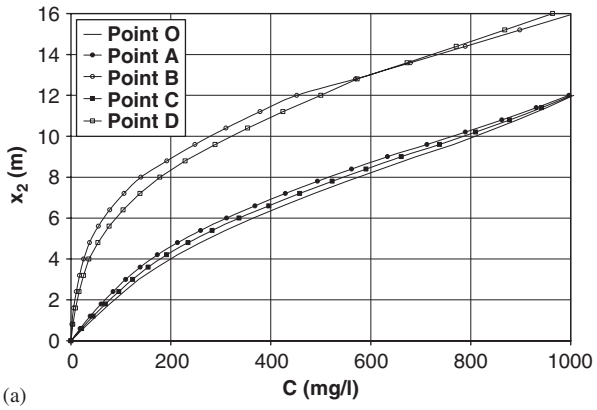

(a)

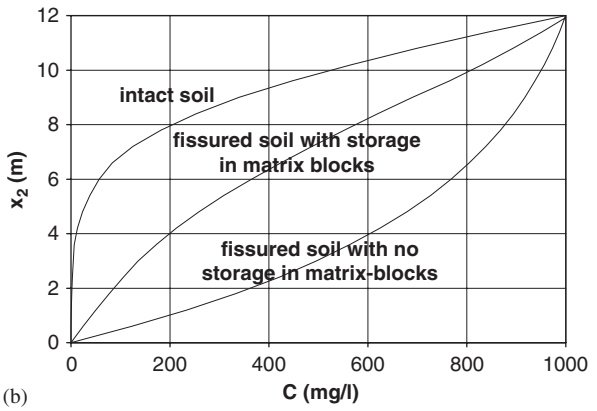

(b)

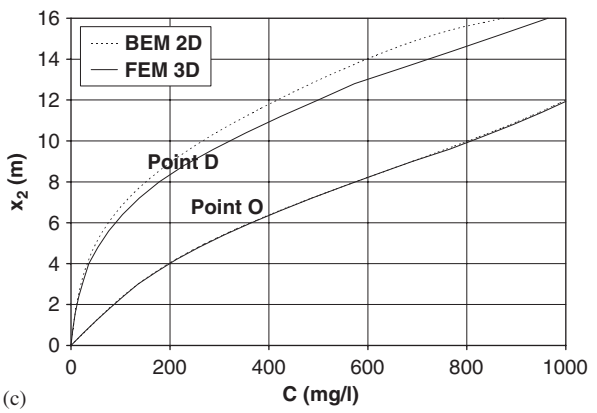

(c)

Figure 10. Problem 3, vertical concentration profiles after 500 years at various points of the landfill (profiles at points *O*, *A*, *B*, *C* and *D* are shown for the 3D analysis; profiles at points *O* and *D* are shown for the 2D analysis; definitions of points are given in Figure 8(a) for the 2D analysis and in Figure 8(c) for the 3D analysis): (a) profiles at various points beneath the landfill; (b) effects of fissures and storage in matrix blocks: profiles at point *O*; and (c) effects of three-dimensional transport: profiles at two points beneath the landfill from 2D and 3D analyses.

Copyright © 2005 John Wiley & Sons, Ltd.

between the clay and the sand are assumed to be nil. Concentration of pollutant in the landfill is 1000 mg/l. Zero-flux boundary conditions are taken at all other surfaces of the landfill. The objective of the analysis is to answer two questions:

1. how does fissuring in the underlying clay affect pollution plumes?
2. to what extent do two-dimensional concentration profiles deviate from three-dimensional ones at various points underneath the landfill?

A preliminary convergence analysis has been conducted to determine the degree of mesh refinement required. The mesh finally used in the analysis is shown in Figure 9. Figure 10 shows vertical profiles of concentration at various points beneath the landfill. In addition, solution from a boundary-element model of the equivalent two-dimensional problem is computed, where the dimensions of the landfill in the x_3 direction are assumed to be much greater than that of the x_1 and x_2 directions. Finally, results from two additional three-dimensional analyses are shown to highlight the effects of fissuring and of storage in the matrix-blocks. The 'no-storage' case is identical to the problem described here except that $D_b \approx 0$, hence removing the storage capacity of the intact soil blocks. The no-fissure case simulates diffusion-only transport in the intact clay soil ($D_{a1} = D_{a2} = D_{a3} = 3.171 \times 10^{-10}\,\mathrm{m^2/s}, v_{a1} = v_{a2} = v_{a3} = 0, n_m = 0.4$).

Figure 10(a) shows vertical profiles of contamination from CONFEM-3D analyses at various locations beneath the landfill. In the lateral directions, concentrations are, as expected, highest close to the centre of the landfill. Figure 10(b) clearly shows that fissuring leads to faster transport in the soil. The slope of the profile at $x_2 = 0$ is an indicator of the magnitude of the flux in the x_2 direction and, therefore, of the amount of contaminants migrating into the groundwater. Comparing the slopes of the profiles from 3D analyses at point O, with and without fissuring, it becomes clear that, after 500 years, far more landfill leachate is reaching the groundwater in the case of the fissured soil. The profile of contaminants at point O, under the scenario of very slow diffusion into the matrix blocks ($D_b \approx 0$), clearly illustrates the importance of taking storage into account in the analysis of fissured soils. Figure 10(c) compares 2D and 3D predictions at points O and D. Under the centre of the landfill, 2D models are clearly accurate. However, discrepancies between 2D and 3D predictions occur under the sloping edge of the landfill (point D). It is worth noting that the 2D concentration predictions under point D are smaller than 3D predictions. This may be due to the proximity of point D to an inclined edge acting as an extra source of contaminants that is not accounted for in 2D analyses.

CONCLUSIONS

The proposed three-dimensional finite-element method can solve a wide variety of soil contamination problems. Its ability to represent fissured soils using an economical multiple-porosity approach, as well as immobile solutions, non-equilibrium sorption and combinations of these problems, makes it particularly useful as a mathematical basis for finite-element software that is general in scope. Numerical experiments showed that the vertical concentration profiles under the sloping edge of a landfill, as calculated by simplified two-dimensional models, can be smaller than more accurate three-dimensional predictions.

Copyright © 2005 John Wiley & Sons, Ltd.

APPENDIX A

A.1. Fissured soils: rectangular blocks

Expressions for η have been derived by Rowe and Booker [33, 34] in the Laplace domain for a set of fissures running between rectangular blocks.

For $n_f = 1$

$$\bar{\eta} = n_b R_b \left[1 - 2 \sum_{i=1}^{\infty} \left\{ \frac{s + \lambda_b}{s + \lambda_b + \dfrac{D_b}{R_b} \alpha_i^2} \frac{1}{(\alpha_j H_1)^2} \right\} \right]$$

For $n_f = 2$

$$\bar{\eta} = n_b R_b \left[1 - 4 \sum_{i,j=1}^{\infty} \left\{ \frac{s + \lambda_b}{s + \lambda_b + \dfrac{D_b}{R_b} (\alpha_i^2 + \beta_j^2)} \frac{1}{(\alpha_i H_1)^2} \frac{1}{(\beta_j H_2)^2} \right\} \right]$$

For $n_f = 3$

$$\bar{\eta} = n_b R_b \left[1 - 8 \sum_{i,j,k=1}^{\infty} \left\{ \frac{s + \lambda_b}{s + \lambda_b + \dfrac{D_b}{R_b} (\alpha_i^2 + \beta_j^2 + \gamma_k^2)} \frac{1}{(\alpha_i H_1)^2} \frac{1}{(\beta_j H_2)^2} \frac{1}{(\gamma_k H_3)^2} \right\} \right]$$

$$\alpha_i = \frac{\pi \left(i - \dfrac{1}{2} \right)}{H_1}, \quad \beta_j = \frac{\pi \left(j - \dfrac{1}{2} \right)}{H_2}, \quad \gamma_k = \frac{\pi \left(k - \dfrac{1}{2} \right)}{H_3}$$

A.2. Structured soils: spherical blocks

Expressions for η have been derived by Huyakorn *et al.* [35] in the Laplace domain for a set of macro-pores surrounded by spherical soil-matrix blocks

$$\bar{\eta} = \frac{3 n_b D_b}{r_0} \left[\chi_b \coth(\chi_b r_0) - \frac{1}{r_0} \right]$$

$$\chi_b = \sqrt{\frac{s R_b}{D_b}}$$

ACKNOWLEDGEMENTS

The project has been supported by a Discovery Grant from the Australian Research Council.

Copyright © 2005 John Wiley & Sons, Ltd.

REFERENCES

1. Rowe RK, Quigley RM, Booker JR. *Clayey Barrier Systems for Waste Disposal Facilities*. Chapman & Hall: London, 1995.
2. Rhyner CR, Schwartz LJ, Wenger RB, Kohrell MG. *Waste Management and Resource Recovery*. CRC Press: Boston, 1995.
3. Biot MA. General solutions of the equations of elasticity and consolidation for a porous material. *Journal of Applied Mechanics* 1956; **23**:91–96.
4. Neretnieks I. Diffusion in the rock matrix: an important factor in radionuclide retardation. *Journal of Geophysical Research* 1980; **85**(B8):4379–4397.
5. Grisak GE, Pickens JF. Solute transport through fractured media: 1. The effect of matrix diffusion. *Water Resources Research* 1980; **16**:719–730.
6. Brusseau ML. Application of a multi-process nonequilibrium sorption model to solute transport in a stratified porous medium. *Water Resources Research* 1991; **27**:589–595.
7. Coats KH, Smith BD. Dead-end pore volume and dispersion in porous media. *Society of Petroleum Engineers Journal* 1964; **4**:73–84.
8. van Genuchten MTh. A general approach for modeling solute transport in structured soils. *Proceedings of Hydrogeology of Locks with Low Hydraulic Conductivity*, *Memoirs of the International Association of Hydrogeologists* 1985; **17**:513–526.
9. Hatfield K, Stauffer TB. Transport in porous media containing residual hydrocarbon. I: model. *Journal of Environmental Engineering* 1993; **119**:540–558.
10. Hatfield K, Ziegler J, Burris DR. Transport in porous media containing residual hydrocarbon. II: experiments. *Journal of Environmental Engineering* 1993; **119**:559–575.
11. Goltz MN, Roberts PV. Interpreting organic solute transport data from a field experiment using physical nonequilibrium models. *Journal of Contaminant Hydrology* 1986; **1**:77–93.
12. Sudicky EA, McLaren RG. The Laplace transform Galerkin technique for large-scale simulation of mass transport in discreetly fractured porous formations. *Water Resources Research* 1992; **28**:499–514.
13. Tang DH, Frind EO, Sudicky EA. Contaminant transport in fractured porous media: analytical solution for a single fracture. *Water Resources Research* 1981; **17**:555–564.
14. Therrien R, Sudicky EA. Three-dimensional analysis of variably-saturated flow and solute transport in discreetly-fractured porous media. *Journal of Contaminant Hydrology* 1996; **23**:1–44.
15. Barenblatt GI, Zheltov YP, Kochina IN. Basic concepts in the theory of seepage of homogeneous liquids in fissured rocks. *Journal of Applied Mathematical Mechanics* 1960; **24**:1286–1303.
16. Warren J, Root PJ. The behaviour of naturally fractured reservoirs. *Society of Petroleum Engineering Journal* 1963; **3**:245–255.
17. Coats KH, Smith BD. Dead-end pore volume and dispersion in porous media. *Society of Petroleum Engineering Journal* 1964; **4**:73–84.
18. Bibby R. Mass transport of solutes in dual-porosity media. *Water Resources Research* 1981; **17**:1075–1081.
19. Shamir UY, Harleman DRF. Numerical solutions for dispersion in porous mediums. *Water Resources Research* 1967; **3**:557–581.
20. Gupta SK, Tanji KK. A three-dimensional Galerkin finite element solution of flow through multiaquifer system. *Water Resources Research* 1976; **20**:553–563.
21. Frind EO, Verge MJ. Three-dimensional modeling of groundwater flow systems. *Water Resources Research* 1978; **14**:844–856.
22. Huyakorn PS, Jones BG, Andersen PF. Finite element algorithms for simulating three-dimensional groundwater flow and solute transport in multilayer systems. *Water Resources Research* 1986; **22**:361–374.
23. Rahman MS, Booker JR. Pollutant migration from deeply buried repositories. *International Journal for Numerical and Analytical Methods in Geomechanics* 1989; **13**:37–51.
24. Zou S, Xia J, Koussis AD. Analytical solutions to non-Fickian subsurface dispersion in uniform groundwater flow. *Journal of Hydrology* 1996; **179**:237–258.
25. Therrien R, Sudicky EA. Three-dimensional analysis of variably-saturated flow and solute transport in discreetely-fractured porous media. *Journal of Contaminant Hydrology* 1996; **23**:1–44.
26. Elzein A, Booker JR. Groundwater pollution by organic compounds: a three-dimensional solution of contaminant transport equations in stratified porous media with multiple non-equilibrium partitioning. *International Journal for Numerical and Analytical Methods in Geomechanics* 1999; **23**:1733–1762.
27. Elzein A. Contaminant transport in fissured soils by three-dimensional boundary elements. *International Journal of Geomechanics* 2003; **3**:75–83.
28. Sudicky EA. The Laplace transform Galerkin technique: a time-continuous finite element theory and application to mass transport in groundwater. *Water Resources Research* 1989; **25**:1833–1846.
29. Sudicky EA. The Laplace transform Galerkin technique for efficient time-continuous solutions of solute transport in dual-porosity media. *Geoderma* 1990; **46**:209–232.

Copyright © 2005 John Wiley & Sons, Ltd.

30. Elzein A. A multiple-porosity model for the transport of reactive contaminants in fractured unsaturated soils with non-equilibrium partitioning. *International Journal of Geomechanics* 2003; **3**(1–2):75–83.
31. Elzein A, Carter JC. A multiple-porosity finite element model for reactive contaminants in soils. *Second MIT Conference on Computational Fluid and Solid Mechanics*, Cambridge, MA, June 2003.
32. Elzein A, Carter JC, Airey DW. Multiple-porosity contaminant transport by the finite-element method. *International Journal of Geomechanics* 2003; **5**(1):24–36.
33. Rowe, Booker JR. A semi-analytic model for contaminant migration in a regular two- or three-dimensional fissured network: conservative contaminants. *International Journal for Numerical and Analytical Methods in Geomechanics* 1989; **13**:531–550.
34. Rowe RK, Booker JR. Contaminant migration in a regular two- or three-dimensional fissured network: reactive contaminants. *International Journal for Numerical and Analytical Methods in Geomechanics* 1990; **14**:401–425.
35. Huyakorn PS, Lester BH, Mercer JW. An efficient finite element technique for modelling transport in fractured porous media, 1. Single species transport. *Water Resources Research* 1983; **19**:841–854.
36. Zienkiewicz OC, Taylor RL. *The Finite Element Method. Volume 1. The Basis* (5th edn). Butterworth and Heinemann: Oxford, 2000.
37. Talbot A. The accurate numerical integration of Laplace transforms. *Journal of the Institute of Mathematics and its Applications* 1979; **23**:97–120.

Copyright © 2005 John Wiley & Sons, Ltd.